ELSEVIER

Ceramics International 31 (2005) 499–505

CERAMICS INTERNATIONAL

www.elsevier.com/locate/ceramint

# Effect of fluoride ions on the preparation of transparent glass ceramics based on crystallization of barium borates

S.A.M. Abdel-Hameed [a,*], N.A. Ghoniem [a], E.A. Saad [b], F.H. Margha [a]

[a] *Glass Research Department, National Research Center, Dokki, Cairo 12622, Egypt*
[b] *Department of Inorganic Chemistry, Faculty of Science, Ain-Shams University, Cairo, Egypt*

Received 25 November 2003; received in revised form 13 April 2004; accepted 28 May 2004

## Abstract

Formation of transparent glass-ceramics based on crystallization of barium borate (BBO) crystals from $BaO\cdot B_2O_3$ glass-systems, with and without addition of $BaF_2$ has been investigated. Crystallization of glass-samples was done by controlled thermal heat-treatment, at nucleation and crystallization temperatures, for different times and rates. When the glasses were heat-treated at the nucleation temperature, transparent glass-ceramics containing 0.1–0.3 μm BBO crystals were prepared. It is obvious that fluorine influences the transparency of glass-ceramics.

*Keywords:* D. Glass ceramics; Nanocrystalline; Transparent; Fluoride; Barium borate

## 1. Introduction

Future applications for glass-ceramics are likely to capitalize on, highly specialized properties for information transmission, display, and storage. Glass-ceramics of uniformly dispersed crystals <100 nm, offer promise for potential new applications [1].

Transparent glass-ceramics generally have two distinctive properties; they are nanocrystalline, and they have greater thermal stability than their parent glasses, frequently having an upper service temperatures of >800 °C [1].

The advantage of transparent and translucent glass-ceramics over polycrystalline light-transmitting substances formed by conventional ceramic processes lies in the capacity and diversity of glass-forming processes. It is also easier to achieve transparency in a polycrystalline material by controlled nucleation and growth of small crystals in glass than by any other ceramic process.

Glass-ceramic materials may transmit visible light if either of the following conditions are operative: (i) the crystallites are much smaller than the wavelength of visible light, or (ii) the optical anisotropy within the crystals and refractive index difference between crystals and glass are very small [2].

Oxyfluoride glass-ceramics are a new hybrid optical material that combines the optical properties of a fluoride crystal and the physical properties of an oxide glass so it can offer the best of both; the low phonon energy of a fluoride and the durability and mechanical properties of an oxide glass [3].

Oxyfluoride glass-ceramics have an advantage over fluoride glasses which, in spite of have been demonstrated as 1.3 μm amplifiers, require a high pump power because of their low quantum efficiency [3]. Fluoride glasses are also expensive, toxic, corrosive and unstable, and must be processed in a dry oxygen-free atmosphere. In addition they have poor durability and are not fusion-spliceable to conventional telecommunications fiber (all of which are $SiO_2$-based), which give rise to device reliability issues that inhibit their use in telecommunications [3].

Oxyfluoride glass-ceramics in which the optically active ion partitions into a fluoride crystal phase offer an economical alternative with substantial performance improvements over fluoride glasses [4].

The β-BBO glass-ceramics have shown a number of interesting properties [5–8]; barium metaborate ($\beta$-$BaB_2O_4$

---

[*] Corresponding author. Fax: +202 3370931.
*E-mail address:* salwa_NRC@hotmail.com (S.A.M. Abdel-Hameed).

0272-8842/$30.00 © 2005 Published by Elsevier Ltd and Techna Group S.r.l.
doi:10.1016/j.ceramint.2004.05.028

Table 1
Chemical composition of glass samples in wt.%

| Samples | BaO | $B_2O_3$ | $BaF_2$ |
|---|---|---|---|
| $B_1$ | 60.29 | 39.71 | – |
| $B_2$ | 47.42 | 39.03 | 13.55 |
| $B_3$ | 45.65 | 37.57 | 16.77 |

Table 2
Results obtained from DTA curves of the analyzed samples

| Samples | $T_g$ | Onset | Peak | End |
|---|---|---|---|---|
| $B_1$ | 585.71 | 685.71 | 716.055 | 726.58 |
| $B_2$ | 564.06 | 630.71 | 655.96 | 660.02 |
| $B_3$ | 557.45 | 634.42 | 655.34 | 660.77 |

or simply β-BBO) is a non-linear optical crystal with a large effective second harmonic generation coefficient, wide transparency range, broad phase-matched region and high damage threshold [9]. Transparent $BaO{\cdot}B_2O_3$ glass-ceramics prepared by controlled crystallization of the glass of the same composition [5] have a UV cut-off at 220 nm, a refractive index of 1.61 and second harmonic generation (SHG) efficiency 0.01–0.12 times that of urea [10].

Recently, Ding et al. [7] have prepared a β-BBO glass-ceramic from a glass of composition $40BaO{\cdot}45B_2O_3{\cdot}15TiO_2$ using the ultrasonic surface modification method. They observed preferred growth of β-BBO microcrystallites at the glass surface giving rise to a transparent, dense thin film that showed a second harmonic generation signal [11].

The aim of the present work is to prepare transparent glass-ceramic based on crystallization of β-BBO phase from the $BaO{\cdot}B_2O_3$ system and to study the effect of replacement of BaO by $BaF_2$ on the crystallization behavior and transparency of the prepared glass-ceramic.

## 2. Experimental procedure

Reagent grade $H_3BO_3$, $BaCO_3$, and $BaF_2$ were well mixed as powder batches. Table 1 shows the batch compositions tested in the present work.

This mixture was melted at 1100 °C for 2 h in air in a Pt crucible in an electric furnace. The as-cast glass was immediately annealed at 400–500 °C and slowly cooled to room temperature. The annealed glass was colorless and transparent.

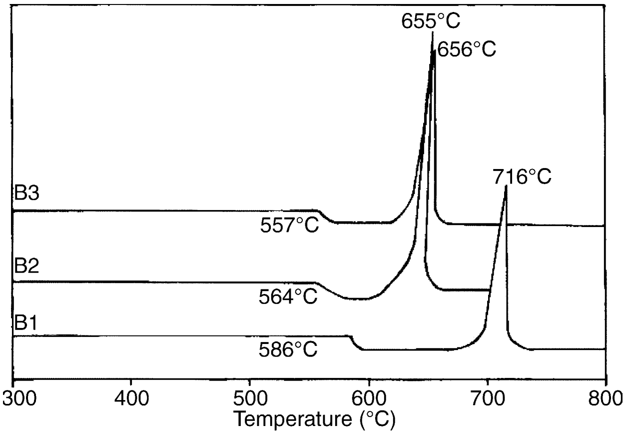

Fig. 1. DTA traces of $B_1$, $B_2$, and $B_3$.

Non-isothermal crystallization of the glasses was studied by differential thermal analysis (DTA). DTA curves were recorded on powdered specimens of about 70 mg under $N_2$ gas at a heating rate of 10 K $min^{-1}$, using a high temperature DTA with $Al_2O_3$ as the reference material. Temperatures detected on DTA curves are accurate to ±2 K. The DTA curves have been obtained using a Perkin Elmer DTA 7 series. The nucleation heat treatments were performed in the DTA apparatus to eliminate temperature gradients. Nucleation times were measured on isothermal DTA curves from the time at which the sample, heated at 50 K $min^{-1}$, reaches the selected temperature.

Identification of crystalline phases was carried out by X-ray diffraction using a diffractometer type Bruker D8 Advance, through examination of fine powders of the glasses, using Cu Kα radiation, before and after heat-treatment.

The surfaces of glass-ceramics samples were examined with a scanning electron microscope (SEM), type JEOL-840A electron probe microanalyzer after coating with gold.

Optical transmission in the UV–vis region was analyzed using a JASCO V350 spectrophotometer using samples of thickness range (0.245–0.29 cm).

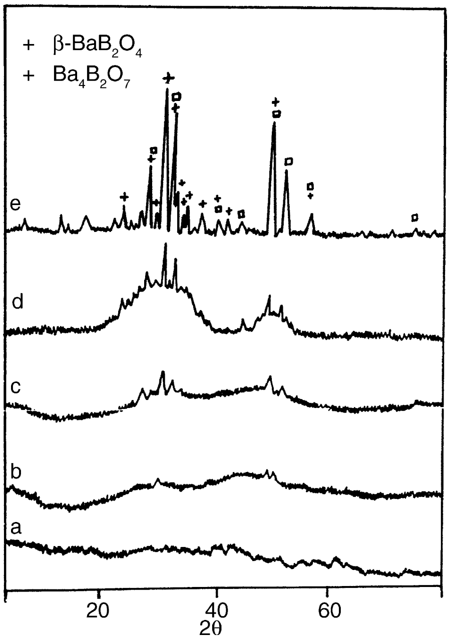

Fig. 2. XRD of $B_1$ as glass (a) and glass-ceramic heat-treated at 550 °C for 15 h (b), 550 °C for 30 h (c), 595 °C for 30 h (d), and 715 °C for 5 min (e).

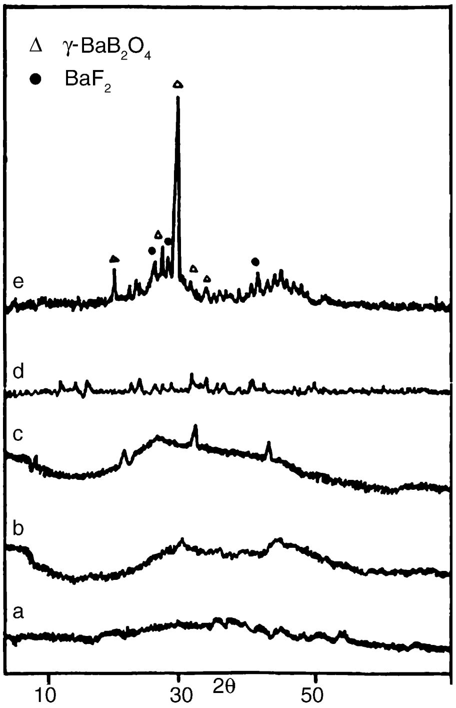

Fig. 3. XRD of glass $B_2$ as glass (a) and glass-ceramic heat-treated at 550 °C for 15 h (b), 550 °C for 30 h (c), 570 °C for 30 h (d)and 655 °C for 5 min (e).

## 3. Results and discussion

The DTA scan provides a rapid way of investigating crystallization, the magnitude of heat effect and the temperature at which it occurs; consequently it is helpful to determine the temperature range of crystallization and the proper heat-treatment schedule.

The DTA traces of all the investigated glasses (Fig. 1) show that the glass transition temperature, $T_g$ is 586 °C for base glass $B_1$. This temperature reduces to 564 °C or 557 °C when BaO is replaced by $BaF_2$ with different quantities as shown in samples $B_2$, $B_3$, respectively. The temperature of maximum crystallization ($T_c$), approximately 716 °C for $B_1$, reduces to ~655 °C for both $B_2$ and $B_3$. Table 2 gives a summary of DTA results.

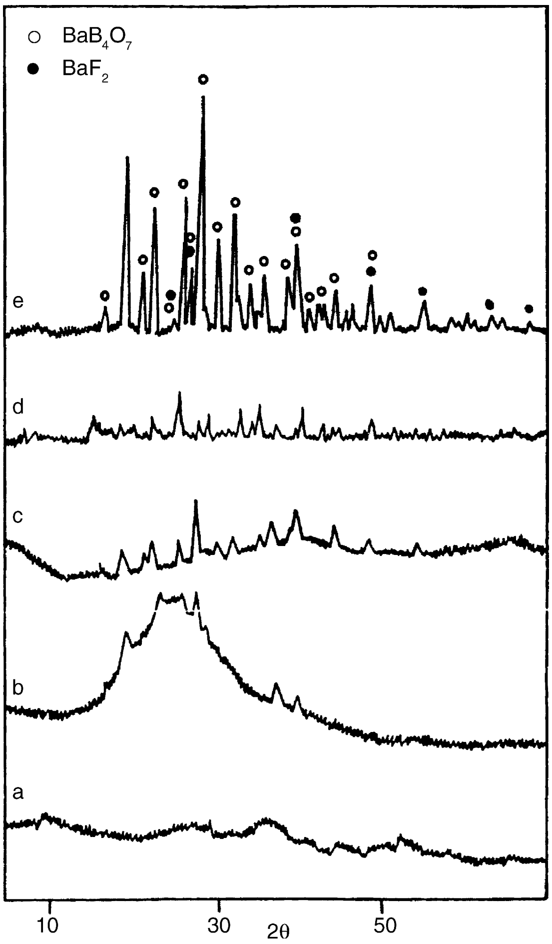

Fig. 4. XRD of glass $B_3$ as glass (a) and glass-ceramic heat-treated at 550 °C for 15 h (b), 550 °C for 30 h (c), 570 °C for 30 h (d), and 655 °C for 5 min (e).

Increasing barium content of Ba in $B_2$ and $B_3$ over $B_1$ leads to a decrease of $T_g$ and $T_c$, these lower temperatures are ascribed to $Ba^{2+}$ ions modifying and weakening the network [12].

Table 3
Phases developed and appearance of glass-ceramics at different heat-treatment schedules

| Sample no. | Heat-treatment parameters (temperature/time) | Rate (°C $min^{-1}$) | XRD results | Appearance |
|---|---|---|---|---|
| $B_1$ | 550 °C/15 h | 10 | Amorphous | Transparent |
| | 550 °C/30 h | 10 | Partial crystallization | Transparent |
| | 595 °C/30 h | 3 | Hemi crystallization | Transparent |
| | 715 °C/5 min | 5 | Holo crystallization of $\beta$-$BaB_2O_4$ + $Ba_4B_2O_7$ | Opaque |
| $B_2$ | 550 °C/15 h | 10 | Amorphous | Transparent |
| | 550 °C/30 h | 10 | Partial crystallization | Transparent |
| | 570 °C/30 h | 3 | Partial crystallization | Transparent |
| | 655 °C/5 min | 5 | Hemi crystallization of $\gamma$-$BaB_2O_4$ + $BaF_2$ | Opaque |
| $B_3$ | 550 °C/15 h | 10 | Partial crystallization | Transparent |
| | 550 °C/30 h | 10 | Hemi crystallization | Transparent |
| | 570 °C/30 h | 3 | Hemi crystallization | Opaque |
| | 655 °C/5 min | 5 | Holo crystallization of $BaB_4O_7$ + $BaF_2$ | Translucent |

It was noticed that the incorporation of different quantities of $F^-$ in the form of $BaF_2$ in $B_2$ and $B_3$ glasses reduces the viscosity of the melts, leading to the reduction of both melting and crystallization onset temperatures [13].

The XRD patterns of all glasses exhibit broad scatter characteristic of the amorphous state as shown in trace (a) in Figs. 2–4. The XRD patterns of all samples, following annealing at the temperature of the DTA exothermic peaks, show crystallization of β-$BaB_2O_4$ + $Ba_4B_2O_7$ for $B_1$, major γ-$BaB_2O_4$ and minor $BaF_2$ for $B_2$ and major $BaB_4O_7$ and minor $BaF_2$ for $B_3$, (trace (b) in Figs. 2–4).

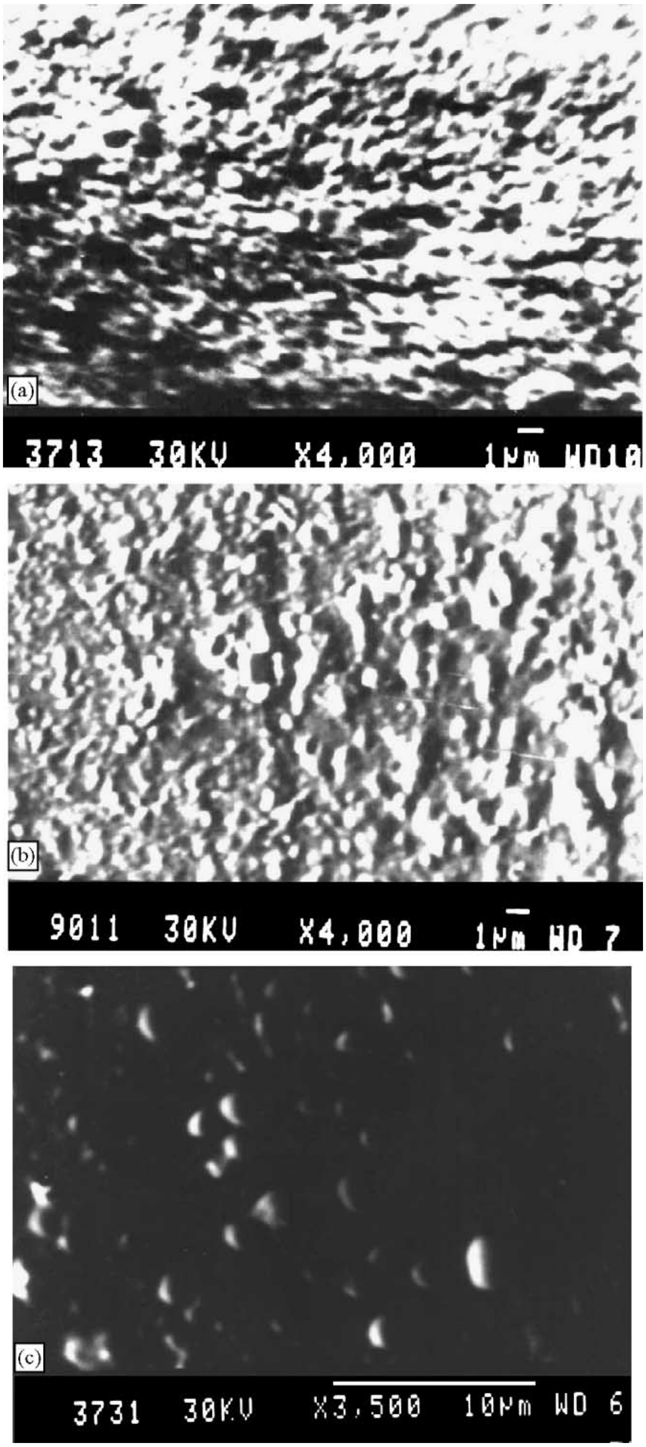

Fig. 5. SEM of (a) $B_1$, (b) $B_2$, and (c) $B_3$ samples heat-treated at nucleation temperature.

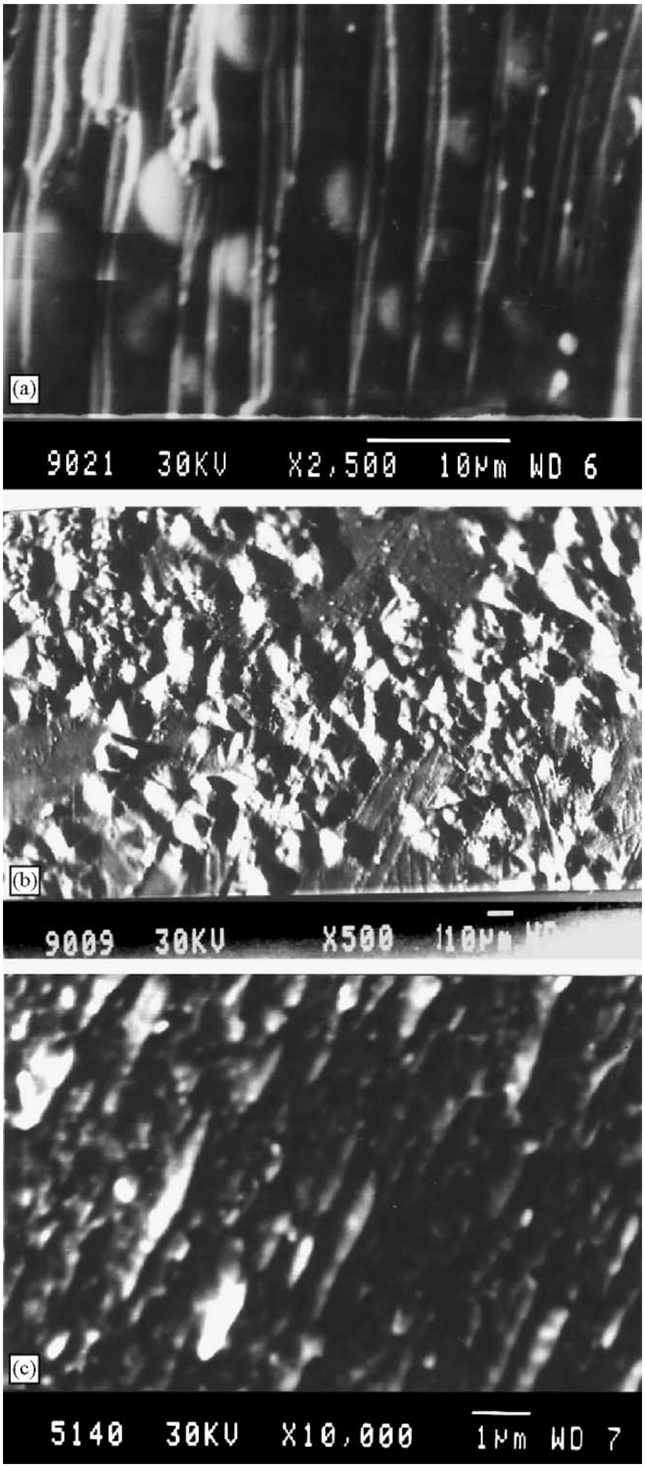

Fig. 6. SEM of (a) $B_1$, (b) $B_2$, and (c) $B_3$ samples heat-treated at crystallization temperature.

Fig. 7. SEM of $B_1$ glass heat-treated at 550 °C for 30 h (350×).

The relative intensity of these lines strongly decreases in the XRD patterns of the samples heated up to the DTA endothermic peak (trace (d) in Figs. 2–4).

Table 3 reveals the phases developed and visual appearance of glass-ceramics, which were prepared using various heat-treatment conditions.

It appears that optical transparency is maintained in samples heat-treated at the nucleation temperature (for times sufficiently short to prevent extensive crystallization and growth). Transparency in these glass-ceramics is assumed to occur due to the presence of crystallites with diameters between 0.1 and 0.3 μm which is in the order of the wavelength of visible light and it can be reasoned on the basis of low crystallite content (Fig. 5a and b) and the lack of crystallites in the center regions of these glass-ceramics [5] (Fig. 5c).

Table 3 shows that transparency is lost after heat-treatment at the crystallization temperature, probably due to the increase of the volume fraction of the heterogeneities $V_h$ (e.g. particles). Growth of the crystallites at this temperature into larger crystallites results in increased scattering of light [5].

Experimental results reveal that after heat-treatment at 550 °C/30 h, the transparent glass-ceramic underwent a significant decrease in the amount of amorphous phase and an accompanying increase in crystalline BBO. After heating at crystallization temperature all the crystalline BBO peaks were visible in the XRD pattern of the non-transparent glass-ceramic (Figs. 2–4).

SEM of optically transparent glass samples heat-treated at the nucleation temperatures for 30 h (Fig. 5); data in Table 3, in general show a uniform ultrafine microcrystalline structure of BBO phases for all samples. Most crystallites diameters are between 0.1 and 0.3 μm. The degree of crystallinity is shown to increase from $B_1$ to $B_2$ (Fig. 5a and b), decreasing with increasing $F^-$ in $B_3$ (Fig. 5c).

The samples heat-treated at crystallization temperature (Fig. 6) show spherical crystallites of β-$BaB_2O_4$ in between fiber bundles of $Ba_4B_2O_7$ crystals in $B_1$ (Fig. 6a), while $B_2$ exhibits coarse grained microcrystalline structure of sub-equihedral pyramid-like crystallites of γ-$BaB_2O_4$ (Fig. 6b). Sample $B_3$ exhibits cryptocrystalline material of crystal size <100 nm of $BaB_4O_7$ when heat-treated at the crystallization temperature (Fig. 6c); its visual appearance is translucent (Table 3).

When $B_1$ samples were heat-treated at temperature (more than nucleation temperature: 550 °C/30 h), transparent glass-ceramics of β-$BaB_2O_4$ spherical like crystallites were obtained (Fig. 7).

Experimental results indicate that $F^-$ has a significant effect on the growth mechanism but a very limited one on the nucleation process, giving rise in almost all cases to non-uniform microstructures (Fig. 6b), It is generally accepted [14] that fluorides, in large amounts, are immiscible in silicate melts leading to glass- in glass phase separation; numerous droplets of one glass dispersed in another are formed. This phase separation decreases the energy barriers necessary for crystallization [15,16]. However, phase separation alone may not be sufficient to induce volume crystallization in the glass and cases are known where glasses having a tendency for phase separation exhibit opalescence during heat-treatment, and do not show volume crystallization [15,16]. However, a uniform ultrafine grained texture was observed in $B_3$ heat-treated at 655 °C/5 min.

Since transparency is an important requirement for glass-ceramics in optical applications, the transmission curves for the prepared transparent glass-ceramics were investigated. Compared with the $B_1$ glass (Fig. 7a), the transmission curves of the heat-treated glass-ceramic of $B_1$ were all slightly shifted toward longer wavelengths.

The spectrum shows that both glass and corresponding glass ceramics of $B_1$ have a transmission cutoff in the UV region at 240 nm (Fig. 8a), but are highly transparent in the visible. Fifty percent transmission occurs at approximately 315 nm and >90% transmission occurs for wavelengths longer than approximately 530 nm. Transparency for crystalline BBO in the UV region is due to the large electronegativity difference in B–O bonds [17]. Like BBO, these $BaO{\cdot}B_2O_3$ glass-ceramics exhibit transparency in the UV region. Their cutoffs at 240 nm remained unchanged from that of the original glass. This cutoff is somewhat higher than that of single crystal BBO at 190 nm [18] comparable to that of urea at 210 nm [18] and shorter than that of KTP at 350 nm [19].

The addition of $F^-$ in the form of $BaF_2$ instead of $O^-$ in $B_2$ is observed to have large effect on the transparency of the heat-treated glass sample, where the transmission curves of both glass and glass-ceramics are identical (Fig. 8b). It is obvious that 50% transmission occurs at approximately 287 nm and >90% transmission occurs for wavelengths longer than approximately 425 nm. Cutoffs in the UV region

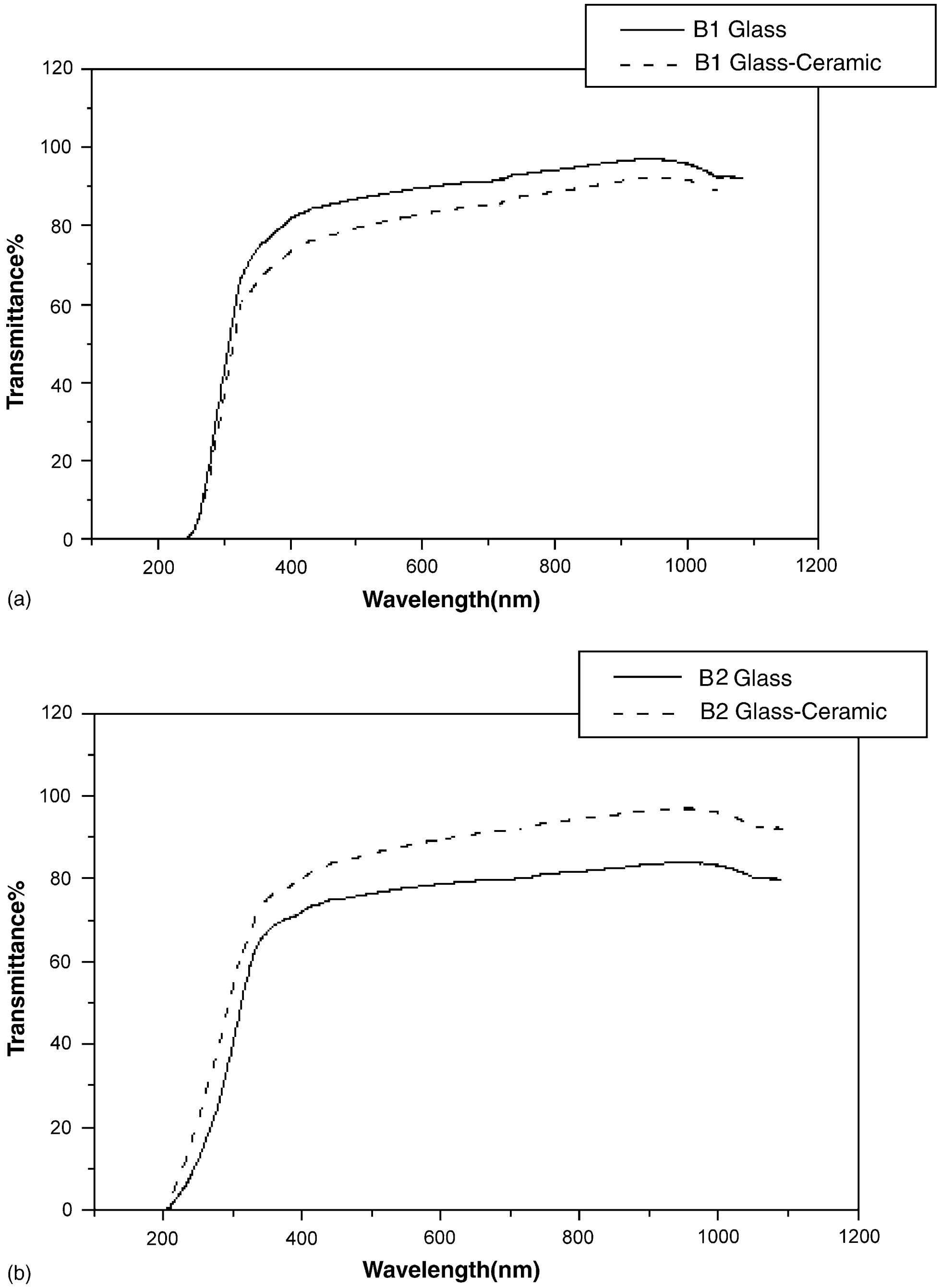

Fig. 8. UV–vis transmission curves of (a) $B_1$ samples (thickness of 0.245 cm) and (b) $B_2$ samples (thickness of 0.29 cm).

are shifted from 240 nm in $B_1$ to 206 nm in $B_2$ and were unchanged from that of the original glass.

## 4. Conclusion

Controlled crystallization of glasses in the system BaO–$B_2O_3$–$BaF_2$, produced transparent BBO glass-ceramics. It is assumed that partial replacing of $O^-$ by $F^-$ facilitates the formation of glass network. It is believed that phase separation in glass is one of the most important factor for the high nucleation rate and consequently for the relatively small grain growth, resulting in the formation of transparent glass-ceramics.

## References

[1] B.H. George, P.R. Linda, J. Am. Ceram. Soc. 82 (1) (1999) 5–16.
[2] G.H. Beall, D.A. Duke, J. Mater. Sci. 4 (1969) 340–352.
[3] D.J. Mtthew, MRS Bull. 23 (11) (1998) 57–62.
[4] D.J. Mtthew, J. Non-Cryst. Solids 239 (1998) 149–155.

[5] Y.H. Kao, Y. Hu, H. Zheng, J.D. Mackenize, K. Perry, G. Bourhill, J.W. Perry, J. Non-Cryst. Solids 167 (1994) 247–254.

[6] Z. Ding, Y. Huany, C. Fang, in: Proceedings of 16th International Congress on Glass, vol. 5, Bol. Soc. Esp. Ceram. Vid., Madrid, 1992, p. 171.

[7] Y. Ding, A. Osaka, Y. Miura, J. Am. Ceram. Soc. 77 (1994) 749.

[8] Y. Ding, A.Y. Miura, A. Osaka, T. Namba, in: Proceedings of the 17th International Congress on Glass, vol. 3, Chinese Ceramic Society, Beijing, 1995, p. 127.

[9] C. Chen, B. Wu, A. Jiang, G. You, Chin. Sci. Sect. B 588 (1984) 604.

[10] P. Pernice, S. Esposito, A. Aronne, V.N. Sigaev, J. Non-Cryst. Solids 258 (1999) 1–10.

[11] P. Pernice, S. Esposito, A. Aronne, Phys. Chem. Glasses 39 (4) (1998) 222–227.

[12] C.B. da Silveira, S.D. de Campos, E.A. de Camposa, A.P.N. de Oliveira, J. Mater. Res. 5 (1) (2002) 1–6.

[13] S.A.M. Abdel-Hameed, Ph.D., Faculty of Science, Ain-Shams University, 2000.

[14] P.W. McMillan, Glass-Ceramics, 2nd Edition. Press, London, 1979.

[15] M.H. Lewis, Glass and Glass Ceramics, Chapman & Hall, London, 1989.

[16] Z. Strand, Glass Science and Technology Series, 8, Elsevier Sci. Pub., 1985.

[17] R.S. Adhav, S.R. Adhav, J.M. Pelaprat, Laser Focus/Electron-Opt. 88 (1987).

[18] C. Chen, G. Liu, Ann. Rev. Mater. Sci. 16 (1986) 203.

[19] G.D. Boyd, H.M. Kasper, J.H. Mcfee, F.G. Storz, IEEE J. Quantum Electron. 8 (1972) 900.